

Student Research Paper  
**Critical clearing time of synchronous generators**

**Author:** [Maximilian Köhler, B. Eng.](#)  
(23176975)

**Supervisor:** Ilya Burlakin, M. Sc.

**Submission date:** March 28, 2024





# Author's declaration

I certify that I have prepared this Student Research Paper without outside help and without using sources other than those specified and that the thesis has not been submitted in the same or a similar form to any other examination authority and has not been accepted by them as part of an examination. All statements that have been copied verbatim or in spirit are marked as such.

Erlangen, March 22, 2024

---

Maximilian Köhler, B. Eng.

## **Note:**

For reasons of readability, the generic masculine is primarily used in this Student Research Paper. Female and other gender identities are explicitly included where this is necessary for the statement.



## **Abstract**

---

Abstract in english.

## **Kurzfassung**

---

Kurzfassung in deutscher Sprache.



# Contents

List of figures	IX
List of tables	IX
<b>1 Introduction</b>	<b>1</b>
<b>2 Fundamentals</b>	<b>3</b>
2.1 Basics synchronous generators . . . . .	3
2.2 System stability esp. transient context . . . . .	4
2.3 Analytical calculation of the critical clearing time . . . . .	6
2.4 Numerical methods for system modeling . . . . .	7
<b>3 Numerical modeling</b>	<b>9</b>
3.1 Structure of the CCT assessment . . . . .	9
3.2 Electrical simplifications and scenario setting . . . . .	9
3.2.1 Electric networks . . . . .	9
3.2.2 Simulation cases and boundaries . . . . .	12
3.2.3 Initial value calculation . . . . .	12
3.3 Implementation of the time domain solution . . . . .	13
3.4 Implementation of the equal area criterion . . . . .	14
<b>4 Results</b>	<b>15</b>
4.1 Analytical results . . . . .	15
4.2 Numerical results . . . . .	15
4.2.1 Simulated faults . . . . .	15
4.2.2 Parameter influence analysis . . . . .	18
4.3 Discussion . . . . .	19
4.4 Limitations . . . . .	19
<b>5 Summary and outlook</b>	<b>21</b>
Acronyms	IX
Symbols	IX
Bibliography	XI
Appendix	23





# List of figures

---

2.1	Types of synchronous generators (SGs) . . . . .	3
2.2	Representative circuit of a single machine infinite bus (SMIB) model . .	5
2.3	Illustrated equal area criterion (EAC) in the P- $\delta$ -curve where $A_{acc} = A_{dec}$	6
3.1	Program plan proposal for determining the critical clearing time (CCT) .	10
3.2	Electrical networks for simulation . . . . .	10
3.3	Simplified electrical networks . . . . .	11
4.1	Power angle plot of fault 3 . . . . .	16
4.2	Power difference behavior over time for fault 2 . . . . .	17
4.3	Influence of parameter variation on the CCT . . . . .	19

# List of tables

---

4.1	Analytical results for the two clearing fault-scenarios . . . . .	15
4.2	Numerical results for CCT-calculations . . . . .	15

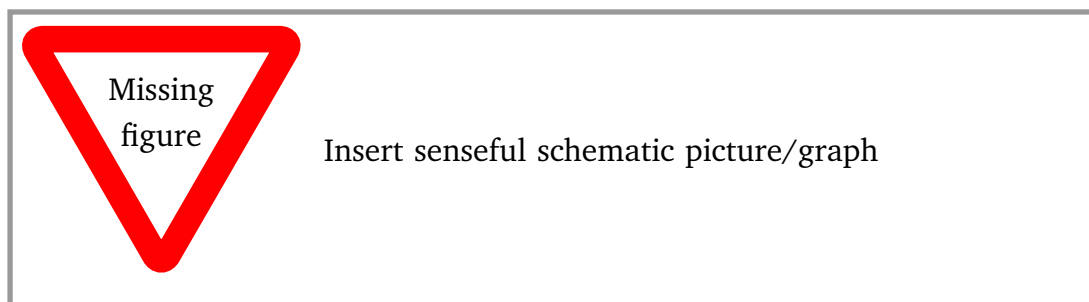


# 1 Introduction

Bullet points for the thesis from Ilya:

- Swing equation of synchronous generators
- Solving the Swing equation with the help of Python -> Solving of second order ODEs
- Equal-area criterion -> Derivation of the equations
- Simulation of a fault -> applying the equal-area criteria with the help of Python.
- Comparison between analytical and (numerical) simulation results

Introduction via [1] and other standard literature like [2]–[6]. Need for understanding of Transient stability and therefore critical pole angle and fault clearing time assessment: Running and maintaining the electrical grid; Adding virtual inertia in FACTs and HVDC; Better and faster predicting, due to shorter (critical) fault clearing times; .



The goal of this Student Research Paper is the implementation of a [CCT](#) determining Python algorithm for a [SMIB](#) model. Therefore a handful of faults or fault scenarios shall be simulated with the program. In combination with a few visualizations the concepts of transient stability assessment, and therefore determining the [CCT](#) and the critical power angle, are illustrated.



## 2 Fundamentals

The sections 2.1, 2.2, 2.4 of the following chapter are recitations of various fundamental literature [3]–[9]. Paragraphs specifically from selected sources are marked as such.

### 2.1 Basics synchronous generators

Synchronous generators (SG) are used for electric power generation and thus connected to a mechanical power or torque input. For power plants most of the time this is a (steam) turbine. The main two types are the high-speed generator (often turbogenerator) and the low speed generator (see Figure 2.1). [4], [5]

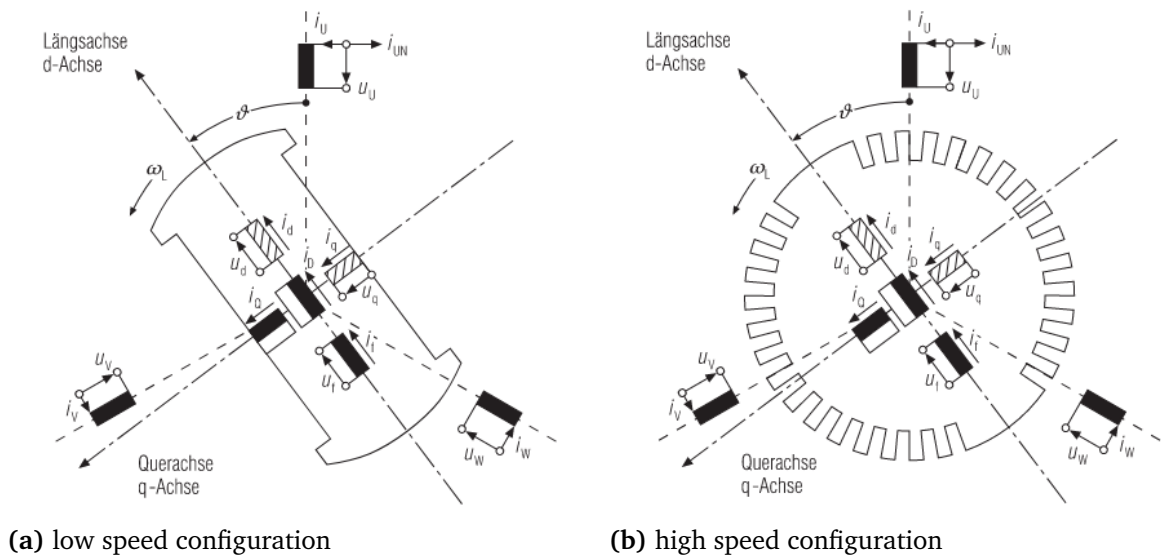


**Figure 2.1:** Schematic view of types of synchronous generators (SGs); from [5]

Generators have a static part, the stator, and the moving rotor. The magnetic windings in the rotor are excited with an excitation voltage, the rotor is then turning inside the stator with the power of the turbine. In the stator a three phase current is injected and can be used for delivering electrical power to a connected grid. The whole principle is a balance between the electromagnetic forces, if the demanded power connected to the stator is too high, the rotor will slow down and vice versa. Usually these generators have so called damper windings, which damp this dynamic behavior. For this research paper, the damping effect is neglected. As well the regulation of the excitation voltage is seen as too complex for this paper. Further information is given in the sources [3]–[6].

Relevant for this paper is the so called swing equation, which is describing the dynamic behavior of the [SG](#).

The final swing equation system can be derived to following two equations, which have to be solved in every time step to determine the pole angle  $\delta$  and the rotor speed  $\omega$ , respectively the rotor speed change from its base value  $\Delta\omega$ :

$$\frac{d\delta}{dt} = \Delta\omega \quad (2.1)$$

$$\frac{d\Delta\omega}{dt} = \frac{1}{2 \cdot H_{\text{gen}}} \cdot (P_{\text{m}} - P_{\text{e}}) \quad (2.2)$$

where

$\delta$	power angle
$\Delta\omega$	change of rotor angular speed
$H_{\text{gen}}$	inertia constant of the <a href="#">SG</a>
$P_{\text{m}}$	mechanical power of the turbine
$P_{\text{e}}$	electrical power demanded transferred out of the <a href="#">SG</a>

## 2.2 System stability esp. transient context

- What is to be analyzed? And why? -> different stability analysis
- rotor angle stability,
- **derivation of EAC**,
- basic assessment models (single machine infinite bus, see [3])

With respect to the limitations, that

1. the machine is operating under balanced three-phase positive-sequence conditions,
2. the machine excitation is constant,
3. the machine losses, saturation, and saliency are neglected,

a simplified single machine infinite bus (SMIB) model can be considered for transient stability assessment (see Figure 2.2). The infinite bus bar (IBB) is working with a constant voltage  $E_{ibb}$  and angle  $\delta_{ibb}$ , typically set to  $0^\circ$ . The real power flowing from the SG to the IBB is then expressed within the Equation 2.3 and only dependent on the power angle  $\delta$ . The reactance  $X_{res}$  is expressing the simplified reactance from the respective circuit.

$$P_e = \frac{E_p \cdot E_{ibb}}{X_{res}} \cdot \sin(\delta) \quad (2.3)$$

The mechanical power of the turbine is assumed constant, due to the short occurrence of transient stability problems.

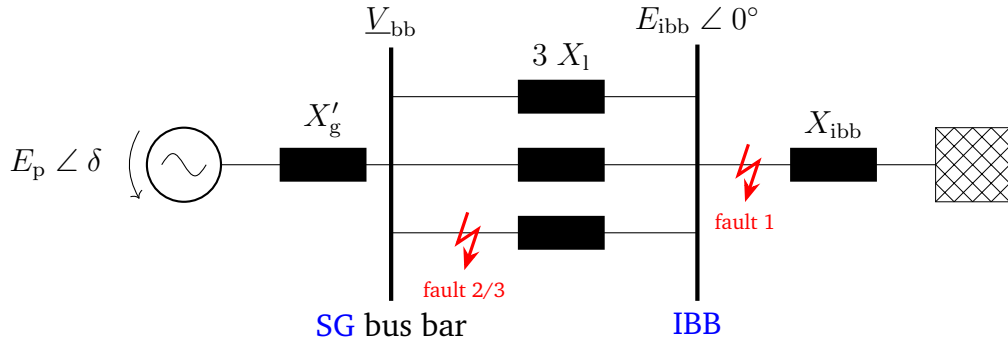


**Figure 2.2:** Representative circuit of a single machine infinite bus (SMIB) model with pole wheel voltage  $E_p \angle \delta$  and infinite bus bar (IBB) voltage  $E_{ibb} \angle 0^\circ$ ; positions of considered faults 1 to 3 are marked with red lightning arrows

where

- $\delta$  power angle (difference)
- $E_p$  pole voltage of the synchronous generator (SG)
- $X'_g$  reactance of the synchronous generator (SG)
- $X_l$  reactance of a single line
- $X_{ibb}$  reactance of the infinite bus bar (IBB)

## 2.3 Analytical calculation of the critical clearing time

For the analytical solution of the swing equation and following the **CCT**, there is the need to find the critical power angle  $\delta_{cc}$  first. For this, the most common approach is the equal area criterion (**EAC**), considering that the amount of stored energy through acceleration (during the short or failure) is equal to the released energy (decelerating the rotor) when synchronizing again. These both energies can be calculated through the area under the curve of the power difference  $\Delta P = P_m - P_e$ , while the accelerating area is be-

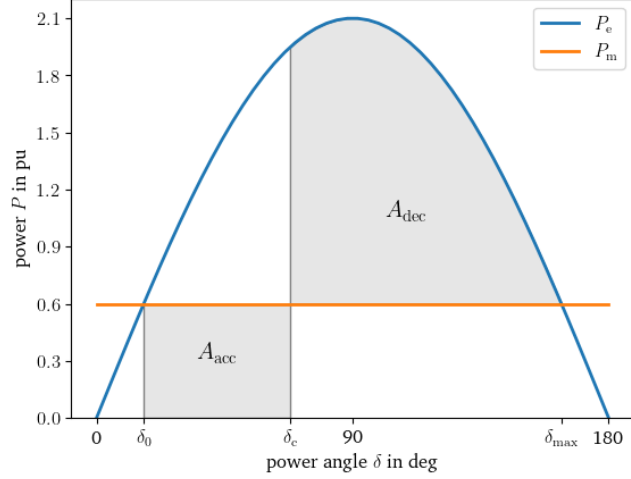


**Figure 2.3:** Illustrated equal area criterion (**EAC**) in the  $P$ - $\delta$ -curve where  $A_{acc} = A_{dec}$

tween the first stable operating angle  $\delta_0$  and the clearing angle  $\delta_c$ , the decelerating area between  $\delta_c$  and the maximum dynamically stable angle  $\delta_{max}$ . **Figure 2.3** is illustrating this approach. Following this approach a generalized expression is formed to

$$\int_{\delta_0}^{\delta_1} \Delta P \, d\delta = 0, \quad (2.4)$$

while the more expressive can be achieved through splitting up the integral borders and equalize both areas:

$$\int_{\delta_0}^{\delta_c} (P_m - P_e) \, d\delta = \int_{\delta_c}^{\delta_{max}} (P_e - P_m) \, d\delta \quad (2.5)$$

With consideration of  $\delta_{max} = \pi - \delta_0$ ,  $P_{e,normal} = P_{max} \cdot \sin(\delta_0)$ ,  $P_{e,fault} = 0$ , and some rearrangements, this leads to the final expression of the critical clearing angle:

$$\delta_{cc} = \arccos \left[ \sin(\delta_0) \cdot (\pi - 2 \cdot \delta_0) - \cos(\delta_0) \right] \quad (2.6)$$



The second step is the calculation of the CCT dependent on the critical clearing angle. Splitting the differentiated variables  $d^2\delta$  and  $dt$  in the combined swing equation and integrating twice, leads to the equation

$$\delta = \frac{\omega \cdot \Delta P}{4H_{\text{gen}}} \cdot t^2 + \delta_0.$$

Rearranging this gives an expression for calculating the critical clearing time  $t_{\text{cc}}$  (see Equation 2.7).

$$t_{\text{cc}} = \sqrt{\frac{4H_{\text{gen}} \cdot (\delta_{\text{cc}} - \delta_0)}{\omega \cdot \Delta P}} \quad (2.7)$$

Both expressions Equation 2.6 and Equation 2.7 are only valid for clearing faults with an electric power drawing of 0 p.u.. For a partial line or power fault, the expressions tend to complicate more. One have to use  $P_e = P_{\text{max, fault}} \cdot \sin(\delta)$  before both integrations of the area equations and the swing equation itself. Finally giving two expressions for the critical power angle  $\delta_{\text{cc}}$  and the CCT  $t_{\text{cc}}$ :

$$\delta_{\text{cc}} = \arccos \left[ \frac{P_m}{P_{\text{max}} - P_{\text{max, fault}}} \cdot (\pi - 2 \cdot \delta_0) - \frac{P_{\text{max, fault}}}{P_{\text{max}} - P_{\text{max, fault}}} \cdot \cos(\delta_0) - \frac{P_{\text{max}}}{P_{\text{max}} - P_{\text{max, fault}}} \cdot \cos(\delta_0) \right] \quad (2.8)$$

$$t_{\text{cc}} = \sqrt{\frac{4H_{\text{gen}} \cdot (\delta_{\text{cc}} - \delta_0)}{\omega \cdot (P - P_{\text{max, fault}} \cdot \sin(\delta_{\text{cc}}))}} \quad (2.9)$$

## 2.4 Numerical methods for system modeling

System dynamics is a method for describing, understand, and discuss complex problems in the context of system theory [SOURCE]. They often can be described through a set of coupled ordinary differential equations (ODEs), most resolved in time dimension. ODEs can be solved through numerical integration with different methods. An easy and less complex method is Euler's method. It uses a linear extrapolation to calculate the functions value at the next timestep, so following the iterable function

$$f_{t+1} = f_t + \left( \frac{df}{dt} \right)_t \cdot \Delta t, \quad (2.10)$$

[MK1]: Sinnvoll da den vollständigen Rechenweg in den Anhang mit aufzunehmen?

[MK2]: Für den zweiten Fall erscheint mir die Berechnung der CCT etwas hoch ->  $P_e$  auch nicht von  $t$  abhängig... Muss ich da einfach statt  $\delta_{\text{cc}}$  die zeitabhängige  $\delta$ -Gleichung einsetzen?

with  $t$  being the time and  $f$  an on  $t$  dependent function. Generally a system of second order ODEs can be rewritten as two first order equations. This often simplifies the calculation or the use of numerical methods. The presented swing equation of a SG in Equation 2.1 and Equation 2.2 has been split up by that principle.

Python is providing a handful of solvers, which can solve such first and second order ODEs. As for this paper, the efficiency and run-time or error of the solver is not in the scope, simply the solver `odeint()` from the package `scipy` is used. The problem is thus explicitly solved.

## 3 Numerical modeling

Following chapter will describe the implementation of Python Code for solving the derived ODE system (see [section 2.1](#)). For this the Python version 3.9 was used, in combination with the packages `scipy`, `numpy`, and `matplotlib`.<sup>1</sup>

### 3.1 Structure of the CCT assessment

The central interest in the algorithm is to determine the time, until a system failure has to be resolved, so that it can remain stable and synchronized. In general, an enough accurate and easy approach for a single machine infinite bus (SMIB) system is the equal area criterion (EAC). For a more complex and coupled machine system, other approaches are more targeting [11]. Further interest is to determine the associated critical clearing angle. This is the maximum possible power angle at the CCT, with which the fault can just be cleared into a stable system. At last one is interested in the time domain solution, just shortly before and after the CCT. This shall illustrate the convergent and divergent behavior of the power angle and therefore the rotor speed.

[Figure 3.1](#) illustrates the rough structure of the numerical calculation. The single processes are further described in [section 3.3](#) for the time resolved solving with `odeint()`, and [section 3.4](#) for the function `determine_cct()`. The iterative solving of stable and unstable regime solutions is, neglecting the fault start and ending as initial conditions, an identical procedure and using the same function set as the described TDS.

### 3.2 Electrical simplifications and scenario setting

#### 3.2.1 Electric networks

The SMIB-model presented in [Figure 2.2](#) has to be divided into the two states *during fault* and *steady state*, and can further be simplified. This leads to a single replacement reactance and is more easy to use in the simulation.

---

<sup>1</sup> documentation and manual can be found on <https://scipy.org/> [10], similar for `matplotlib`, and `numpy` packages

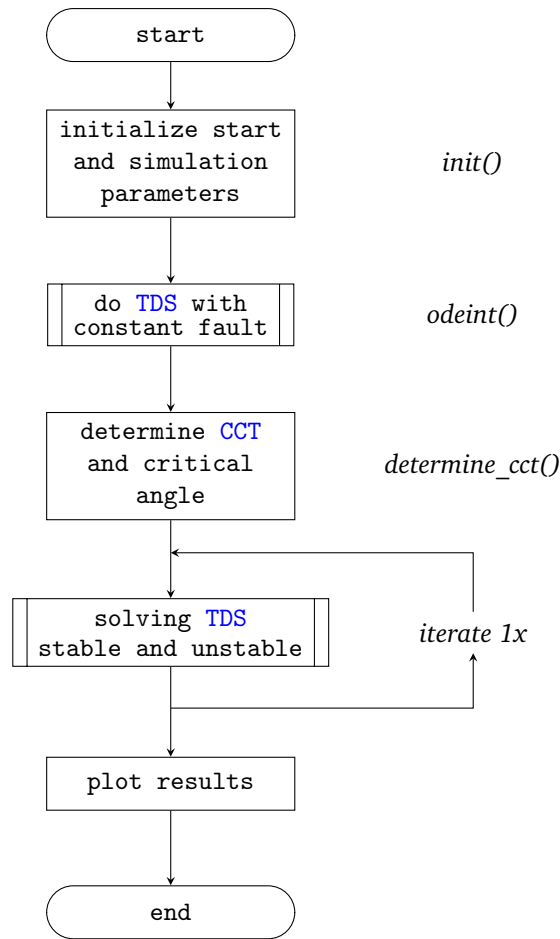


**Figure 3.1:** Program plan proposal for determining the critical clearing time (CCT)  $t_{cc}$ , critical power angle  $\delta_{cc}$  and the time domain solution (TDS) of the single machine infinite bus (SMIB)-model; including the associated main function name

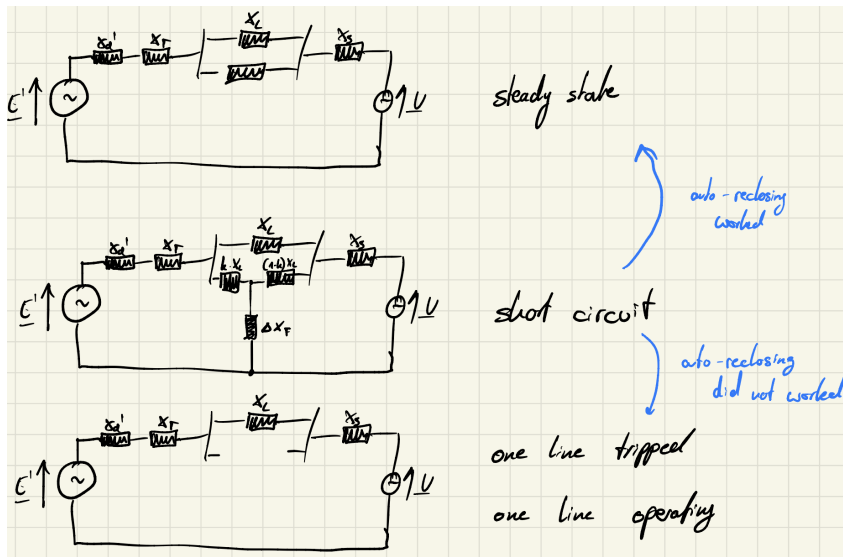


**Figure 3.2:** Electrical networks for simulation

Figure 3.2 shows the steady state circuit, the system during the fault and the possible network after and with no clearing of the fault. Normally the third state is not necessary. The networks in Figure 3.3 are the represented ones in the simulation, the reactances thus have to be simplified for a targeted simulation.

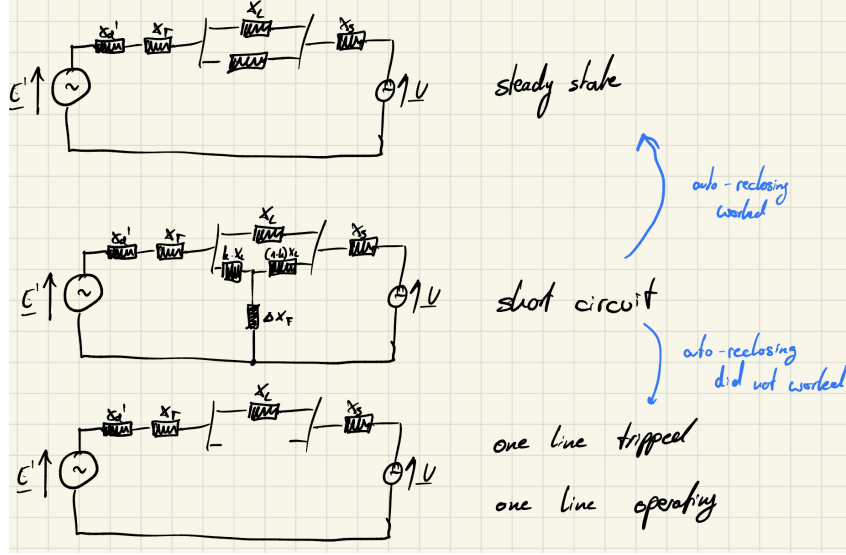


Figure 3.3: Simplified electrical networks

Electrically speaking from the swing equation (Equation 2.2), the real power flowing from the SG to the IBB is to be calculated. With the general equation for the power looking at the generator bus bar

$$P = V \cdot I^*,$$

and ohms law connected with the nodal admittance matrix for the voltage at the bus bar (see Equation 3.3 and 3.2), the only thing left for calculating the power is the injected current from the SG to the generator bus bar. The details we know about the SG help to describe it as a voltage source, but with a transformation it can be used as current source, delivering the injected current at the generator bus bar (see Equation 3.1).

$$I_{inj} = \frac{E}{jX} \quad (3.1)$$

$$V_{bb} = Y_{11} \cdot I_{inj, gen} + Y_{12} \cdot I_{inj, ibb} \quad (3.2)$$

$$I_{bb} = \frac{E_{gen} - V_{bb}}{jX} \quad (3.3)$$

where

$\delta$	power angle (difference)
$E_p$	pole voltage of the synchronous generator (SG)
$X'_g$	reactance of the synchronous generator (SG)
$X_l$	reactance of a single line
$X_{ibb}$	reactance of the infinite bus bar (IBB)

### 3.2.2 Simulation cases and boundaries

The boundaries of the single cases, which are simulated, are given with a Python dictionary. Therefore the values of the variables have to be predefined and documented. Considering fault cases, there are three differences in the interest:

1. A full line fault, meaning the complete electrical power is disconnected. The CCT of the fault has to be determined, a TDS with fault clearing shortly before and after the critical clearing is carried out and displayed as *stable* and *unstable*;
2. A partial line fault, meaning just a defined percentage of the electrical power is disconnected. The further evaluation is carried out like in scenario 1.;
3. A partial line fault, meaning just a defined percentage of the electrical power is disconnected. But with consideration, that the fault condition is stable at a new operation point. This point is calculated in the time domain.

Further of interest is a parameter variation of both influences  $H_{gen}$  and  $\Delta P$ . This last parameter is not meant to describe the absolute power difference, which is inserted into the swing equation, but more the power difference relative to the maximum electrical power output of the generator. Due to the relation between the maximum power output and the disconnected electrical power in the acceleration and deceleration of the rotor, it seems more significant to use this as a relative parameter. The CCT in dependency of these two influences shall be elaborated.

### 3.2.3 Initial value calculation

For the setting of starting values, the per unit system is preferred. Because of the relative nature of this unit, it acts as generalization and can be applied to concrete examples with known nominal sizes. Generally speaking,  $P_{e,max}$ ,  $P_e = P_{mech}$ ,  $E_{ibb}$ ,  $E_{gen}$ ,  $\delta_{ibb}$  and  $\delta_{gen}$  are needed to be predefined for the simulation.

As the point of interest in most calculations, the voltage at the at the **IBB** is set to 1 p.u.. Most of the until now presented equations are referring to power angle differences. For a simplified calculation, it is handsome to set the power angle of the **IBB** to  $0^\circ$ , thus all the power angle and angle developments dependent on the time are solely related to the absolute power angle of the generator. The maximum electrical power of the generator is arbitrarily set to 1.2 p.u., the real power extracted from the generator into the grid node is set to 0.9 p.u.. With these predefinitions and both following equations we can calculate the remaining two values.

$$E_{\text{gen}} = \frac{P_{e,\text{max}} \cdot X}{E_{\text{ibb}} \cdot \sin(90^\circ)} \approx 1.14 \text{ p.u.}$$

$$\delta_{\text{gen}} = \arcsin\left(\frac{P_e \cdot X}{E_{\text{ibb}} \cdot E_{\text{gen}}}\right) \approx 48.6^\circ$$

The reactances for the different fault scenarios can be derived from the electrical networks in [subsection 3.2.1](#). Therefore the general reactance in operation mode is constituted with the reactance of the generator, the line, and the **IBB**. For fault 1 the additional fault reactance is getting very high in addition to the generator, thus it can be neglected. Fault 2, considering just a partial line tripping, is increasing the contribution from the line to  $\frac{3}{2}$  of its initial value. The other contributions stay consistent. For fault scenario 3 the reactances are consistent whether the fault is present or not. The initial electrical power is reduced to 0.6 p.u. and thus the initial power angle of the generator is set to  $30^\circ$ .

A compromised overview of the initial values and the values in the fault cases is given in [section A.1](#).

### 3.3 Implementation of the time domain solution

The **TDS** shall be solved with a python integrated solver, due to the fact that numerical solvin methods are not scope of this paper. The solver `odeint()` from the `scipy`-package is therefore used as preferred algorithm. This requires a time array with all the timesteps of interest and a differential function, which is solved through every time step. Due to the second order nature of the swing-equation and just the possibility to solve first order ones, the equation has to be split up into two first order equations and solved simultaneously. This can be realized via using a solution array instead of a variable.

Looking deeper into the swing equation, both the demanded electrical power from the grid or connected network and the mechanical power put into the roter from the steam turbine have to be calculated at each time step. While the mechnanical power is a

bit easier to calculate, the electrical power is a bit more complex. In order to get a good representation, the algebraic equations describing the connected network (see [subsection 3.2.1](#)), have to be solved at every time step as well. For this a dedicated function *algebraic()* is included.

[MK4]: Include the equation for the mechanical power?

## 3.4 Implementation of the equal area criterion

The equal area criterion (EAC) is computed as the name states. It is comparing the accelerated area with the decelerable area, and therefore comparing the stored to the braking (or re-synchronizing) energy. The main function *deteming\_cct()* is differentiating between clearing and non-clearing mode. First one is taking the pre-fault status of the connected network also as post-fault condition, thus calculating the clearing time and angle the generatr and the network can remain in the fault state. The non-clearing mode is taking the fault condition as post-fault condition and is calculating a new stable power angle convergent.

The main though is iterating through the [TDS](#) at each time step, looking if enough braking reserve is left and saving the current time and angle as solution. If the loop continues, the solution is overwritten. As pre-set the solution is negative. This enables a quick understanding of simulation faults or a general unstable initial condition set.

As a helping function *stability\_eac()* allows a simple check in the loop. It calculates the currently passed acceleration area, and the until the maximum dynamically stable power angle  $\delta_{\max} = \pi - \delta_0$  possible decelerating area, it can compare and state stability or instability at the current time point.

Another possible way would be to check the stability first under the  $P - \delta$ -curve, gathering the critical angle. After that a simple run through the [TDS](#) can deliver the searched [CCT](#). Within this approach the angle spectrum has to be searched in addition to the [TDS](#). This doubled vector searching seemed as easy improvement in comparison to the previous method and was therefore neglected.



# 4 Results

## 4.1 Analytical results

The analytical calculation follows the equations from [section 2.3](#). For fault 1 the simplified ones could be used, the more complex and advanced are needed for fault case 2. Therefore the base values for the first two input scenarios are used like in the numerical simulation. For the third one no CCT is calculatable, due to the stable nature of the fault scenario. The results of this calculation are shown in [Table 4.1](#).

**Table 4.1:** Analytical results for the two clearing fault-scenarios; considering  $\delta_{cc}$  and  $t_{cc}$

scenario	$\delta_{cc}$	$t_{cc}$
fault 1	65.01°	0.116 s
fault 2	93.99°	0.595 s

## 4.2 Numerical results

[Table 4.2](#) is summarizing the results for the CCT-calculation of the different set scenarios in [section 3.2](#). Like in the analytical results section before, the third fault can not be displayed in the context of the first two clearing ones. The maximum reached power angle for fault 3 is 69.3°, while the new stable power angle is around 48.6°. At first the system oscillates around this new angle, until the damping factor results in a new stable and steady operation point.

**Table 4.2:** Results (CCT and  $\delta_{cc}$ ) for numerical solving the faults 1, 2, and 3

scenario	$\delta_{cc}$	$t_{cc}$
fault 1	65.9°	0.119 s
fault 2	95.9°	0.394 s

### 4.2.1 Simulated faults

Looking deeper into the numerical results is possible through plotting the development of the power angle over the time. In addition to that the used energies or respectively areas in the  $P - \delta$ -curves. [Figure 4.1](#) is looking deeper into the non-clearing fault three.

[MK5]: Was ist mit nicht vollständigen Fehlern? Gleichungen für analytical beschreiben nichts...

Because of spacial reasons, the complete plot sets for all faults are included in the [section A.2](#), [section A.3](#) and [section A.4](#).

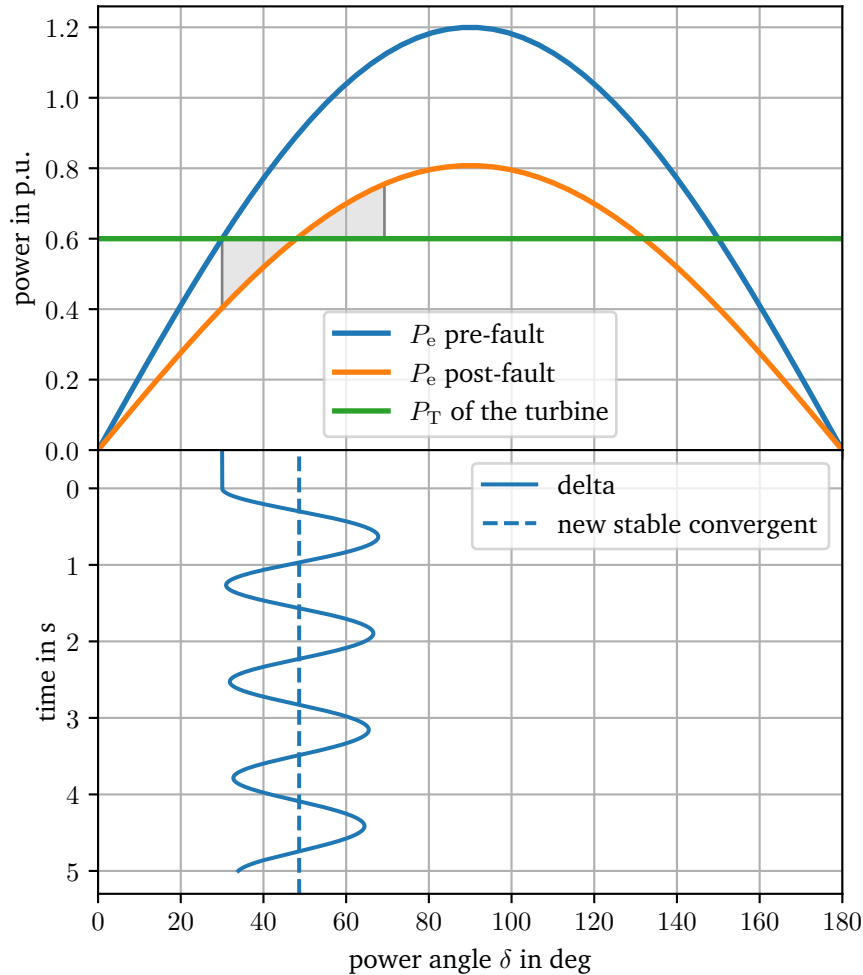


**Figure 4.1:** Power angle plot of fault 3 in time and power domain; grey areas illustrate the used area under the curve for storing and releasing kinetic energy in/out of the rotor

Both partial sinus functions represent the electrical power demanded from the electrical connected network. During the fault, in this case post-fault as well, is lower in the peak and thus giving another intersection point with the straight horizontal mechanical power from the turbine. The new stable convergent is falling together with this intersection point. The used area is reaching from the starting power angle over the post-fault intersection point to the maximum swept power angle in the time resolution. In this case the fault is starting to occur at the time point 0 s.

For fault one and two the whole area until the maximum dynamic stable operation point, the second intersection point with the pre-fault partial-sinoidal wave, is used. Therefore the critical angle is not at the intersection with the during fault electrical power curve. The unstable scenario, clearing the fault just a few time steps after the CCT leads to a divergent power angle. Clearing just in time shows a stable, oscillating behavior, while resulting in a maximum overswing in the region of the maximum dynamic stable power angle. This behavior can be seen in fault one as well as in fault two, while in fault one the static stable angle cannot be reached, in fault two it is even overstepped.

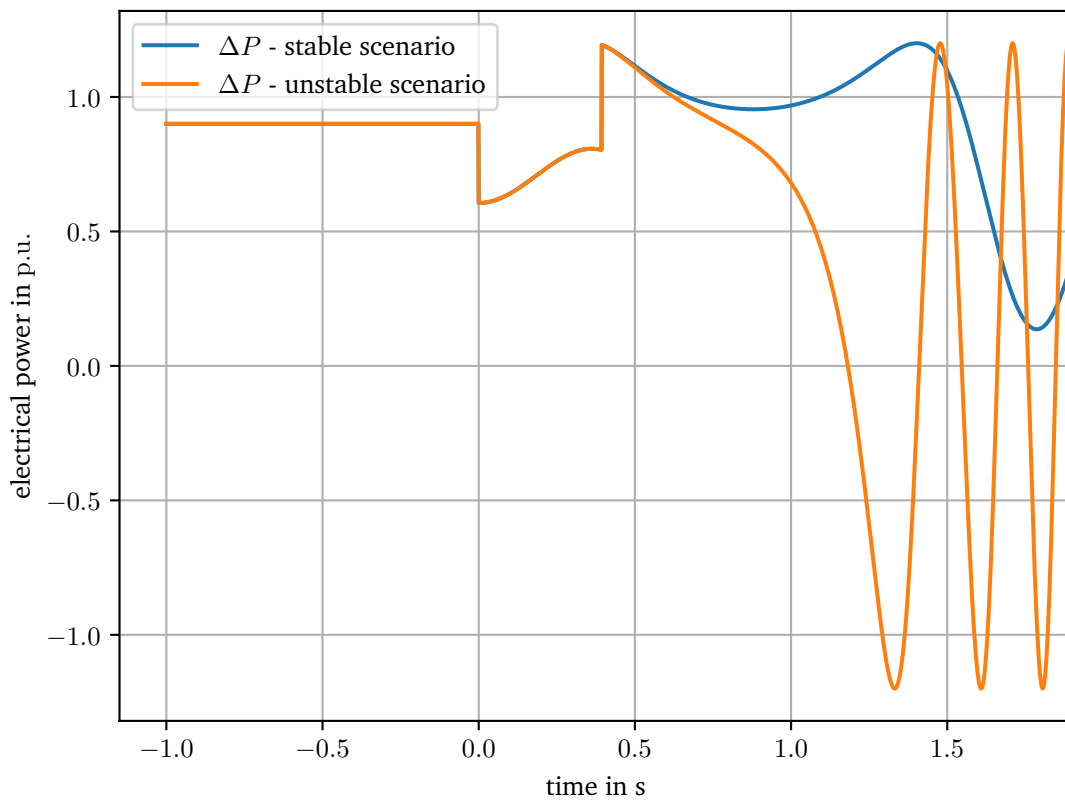


**Figure 4.2:** Power difference behavior over time for fault 2; stable operation mode in negative time regime, fault is occurring between 0 s and 0.394 s

Plotting the electrical extracted power  $P_e$  of fault two against the time the power swings in the stable and the unstable case are visible. While stable operation before the fault occurring, it is on one continuous value. As soon as the line is shorted, the electrical power sinks suddenly down, with the fault duration it is getting bigger again. With clearing the fault another jump is happening to a greater power value than initially in stable operation, followed by an oscillation of the power. While in the stable case the swings have a bigger oscillation period and does not cross into the negative real power regime, the unstable case is swinging relatively fast and showing extreme values ranging

far into the negative regime. A similar result can be seen within the fault one. One exception: the electrical power during the fault is zero, because the line is completely not working and thus, no real power can be extracted from the generator. While fault three is present, a first jump with the fault occurrence is observable. After that, the real power is swinging around the before stable power point. Like in [Figure 4.1](#) illustrated, a new stable operation point given by the new intersection of the power curves with a new stable power angle.

### 4.2.2 Parameter influence analysis

Other variables changing the [CCT](#) of a generator are the power difference  $\Delta P$  and the generator parameter  $H_{\text{gen}}$  (see [Equation 2.2](#)). The resulting [CCT](#) while varying this parameters in the ranges

$$H_{\text{gen}} = [0, 12] \text{ s, and}$$

$$\Delta P = [25, 91.7] \%$$

is shown in [Figure 4.3](#).

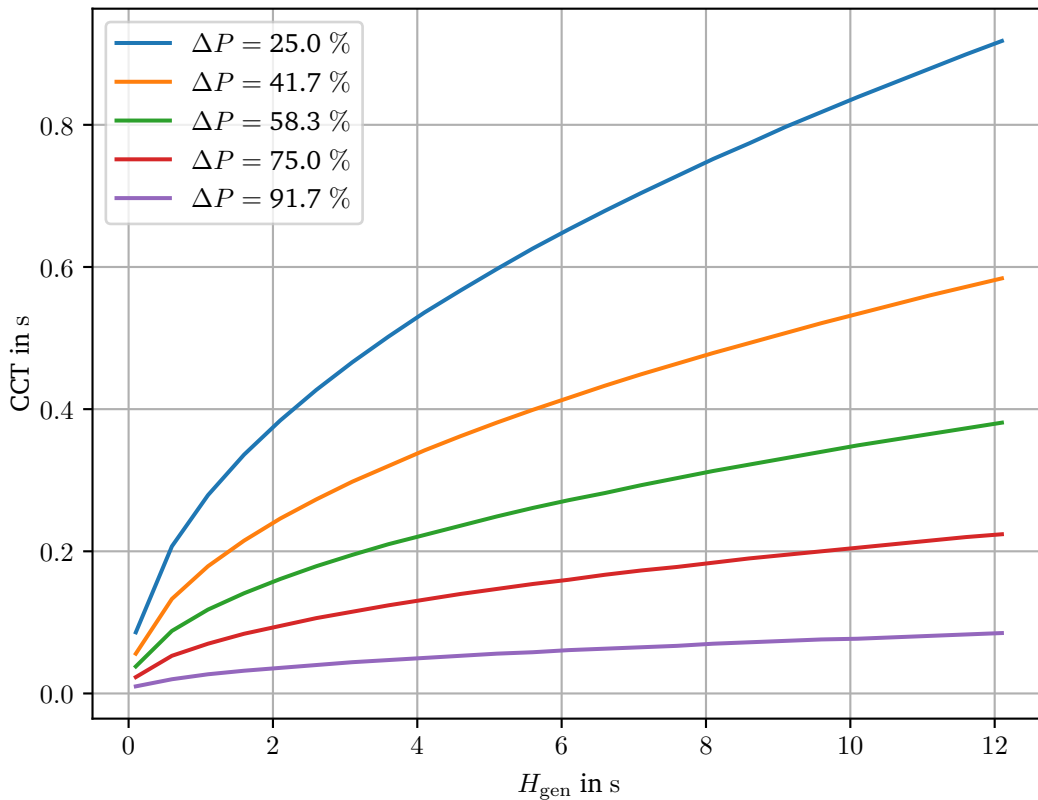


**Figure 4.3:** Influence of varying the parameters power difference  $\Delta P$  and generator parameter  $H_{\text{gen}}$  on the critical clearing time (CCT)

Good visible is the similar progression of the CCT. With increasing  $H_{\text{gen}}$  the CCT is getting bigger as well. The fewer the electrical extracted power is to the maximum electrical power, the bigger the CCT is. This effect is as well non-linear and increasing with a lowering  $\Delta P$ .

## 4.3 Discussion

## 4.4 Limitations

- Just stable or unstable, not metastable (first swing ok, after that unstable development)
- No damping -> new stable point with low oscillation amplitude in fault 3 is not reached within a few seconds

- Simplified generator model, only one generator. No machine interaction considered.  
-> Other algorithms
- Differences: Calculation via TDS and area, via area under the curve solely, stability criteria in the TDS (function  $P(\delta)$  -> find extreme points and compare them with the maximum power angles; Paper from Ilya: [11])

# 5 Summary and outlook

Short summary of the results.

A brief look in the future and why this topic is in the interest, maybe for slightly other applications as well (see [12]).

- Usage of CCT assessment for different topics like: Grid coupling (stations); transient balancing processes (RoCoF?)
- Using of TDS assessment for TSA: controlling of regenerative energy sources like wind turbines; controlling of stability devices like phasor-shifting, grid-forming power electronics
- Support of reactive and real power flow controlling: Slower expansion of transient disturbances through grids for stabilization with (comparably slow) primary control





# Acronyms

---

CCT	critical clearing time
EAC	equal area criterion
IBB	infinite bus bar
ODE	ordinary differential equation
SG	synchronous generator
SMIB	single machine infinite bus
TDS	time domain solution

# Symbols

---

$H_{gen}$	s	inertia constant of a synchronous generator (SG)
$P$	W	Power; electrical or mechanical



# Bibliography

- [1] “Perspektiven der elektrischen Energieübertragung in Deutschland,” VDE Verband der Elektrotechnik Elektronik Informationstechnik e.V., Ed., Frankfurt am Main.
- [2] J. D. Glover, T. J. Overbye, and M. S. Sarma, “Power system analysis & design,” Boston, MA.
- [3] P. S. Kundur and O. P. Malik, *Power System Stability and Control*, Second edition. New York Chicago San Francisco Athens London Madrid Mexico City Milan New Delhi Singapore Sydney Toronto: McGraw Hill, 948 pp., ISBN: 978-1-260-47354-4.
- [4] J. Machowski, Z. Lubosny, J. W. Bialek, and J. R. Bumby, *Power System Dynamics: Stability and Control*, Third edition. Hoboken, NJ, USA: John Wiley, 1 p., ISBN: 978-1-119-52636-0 978-1-119-52638-4.
- [5] D. Oeding and B. R. Oswald, *Elektrische Kraftwerke und Netze*, 8. Auflage. Berlin [Heidelberg]: Springer Vieweg, 1107 pp., ISBN: 978-3-662-52702-3. DOI: [10.1007/978-3-662-52703-0](https://doi.org/10.1007/978-3-662-52703-0).
- [6] A. J. Schwab, *Elektroenergiesysteme: smarte Stromversorgung im Zeitalter der Energiewende*, 7. Auflage. Berlin [Heidelberg]: Springer Vieweg, 871 pp., ISBN: 978-3-662-64773-8.
- [7] S. Georgiev and I. M. Erhan, *Numerical Analysis on Time Scales* (De Gruyter Graduate). Berlin: De Gruyter, 382 pp., ISBN: 978-3-11-078725-2.
- [8] W. Miles, *Numerical Methods with Python: For the Sciences* (De Gruyter Textbook). Berlin ; Boston: De Gruyter, 314 pp., ISBN: 978-3-11-077645-4.
- [9] H. P. Langtangen, *A Primer on Scientific Programming with Python* (Texts in Computational Science and Engineering 6), 5th edition. New York, NY: Springer Berlin Heidelberg, ISBN: 978-3-662-49886-6.
- [10] P. Virtanen, R. Gommers, T. E. Oliphant, *et al.*, “SciPy 1.0: Fundamental algorithms for scientific computing in Python,” *Nature Methods*, vol. 17, no. 3, pp. 261–272, ISSN: 1548-7091, 1548-7105. DOI: [10.1038/s41592-019-0686-2](https://doi.org/10.1038/s41592-019-0686-2). [Online]. Available: <https://www.nature.com/articles/s41592-019-0686-2>.
- [11] S. Batchu, Y. Raghuvamsi, and K. Teeparthi, “A Comparative Study on Equal Area Criterion Based Methods for Transient Stability Assessment in Power Systems,” in *2022 22nd National Power Systems Conference (NPSC)*, New Delhi, India: IEEE, pp. 124–129, ISBN: 978-1-66546-202-0. DOI: [10.1109/NPSC57038.2022.10069303](https://doi.org/10.1109/NPSC57038.2022.10069303). [Online]. Available: <https://ieeexplore.ieee.org/document/10069303/>.

- [12] Z. Gao, W. Du, and H. Wang, “Transient stability analysis of a grid-connected type-4 wind turbine with grid-forming control during the fault,” *International Journal of Electrical Power & Energy Systems*, vol. 155, p. 109 514, ISSN: 01420615. DOI: [10.1016/j.ijepes.2023.109514](https://doi.org/10.1016/j.ijepes.2023.109514). [Online]. Available: <https://linkinghub.elsevier.com/retrieve/pii/S0142061523005719>.

# Appendix

<b>A</b>	<b>Graphics and tables</b>	<b>25</b>
A.1	Initial values . . . . .	25
A.2	Fault 1 . . . . .	26
A.3	Fault 2 . . . . .	29
A.4	Fault 3 . . . . .	32



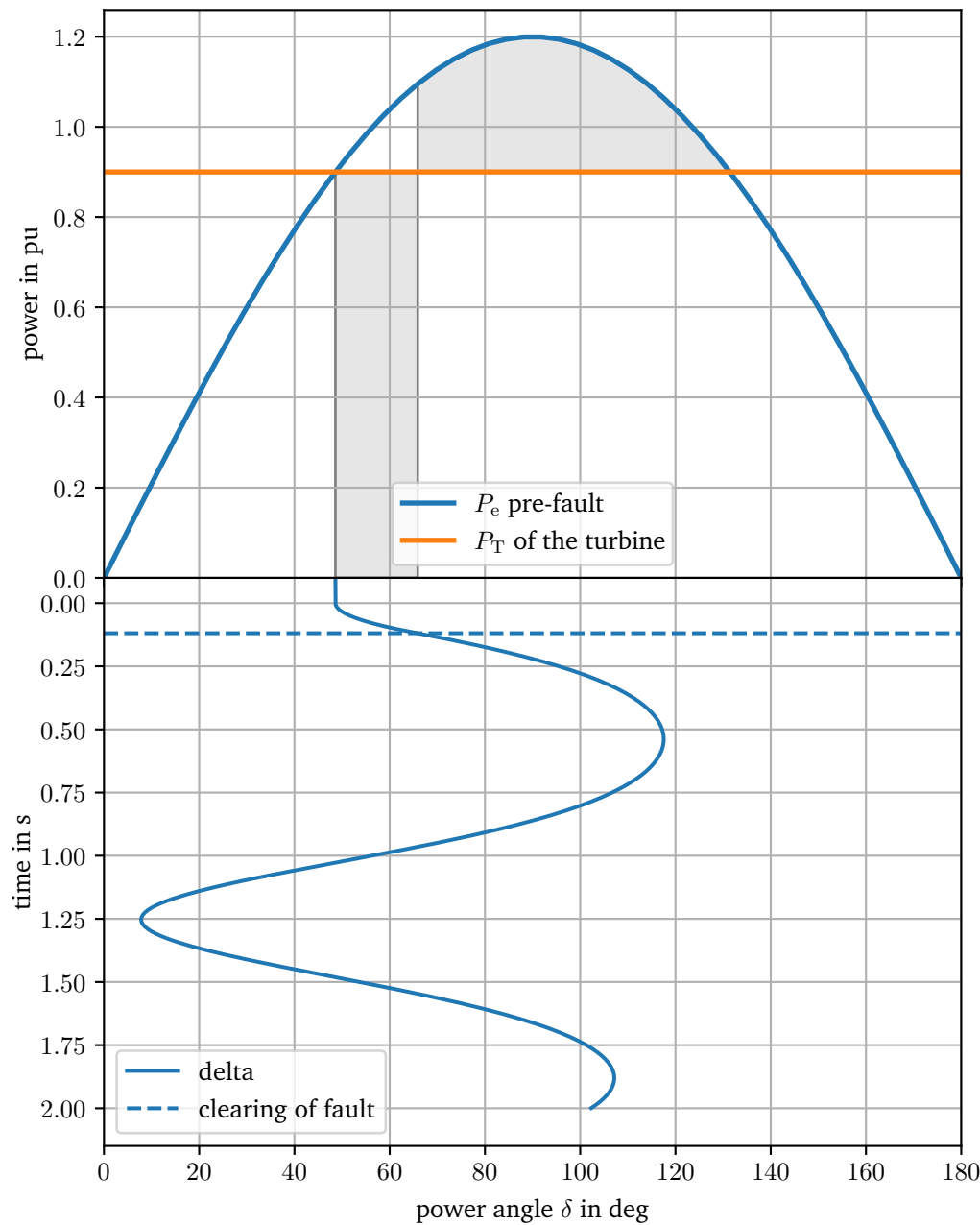
# A Graphics and tables

## A.1 Initial values

a	b

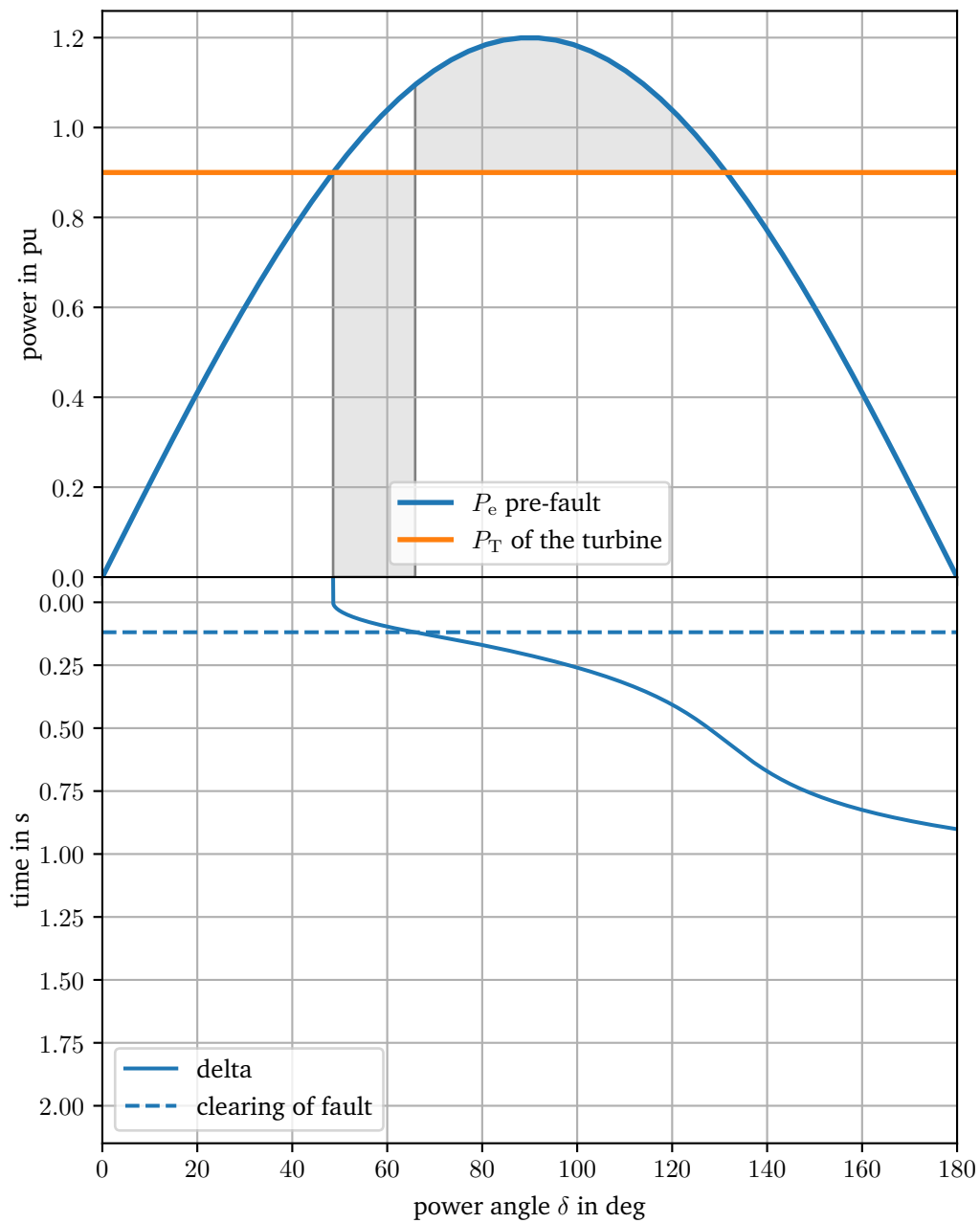
## A.2 Fault 1

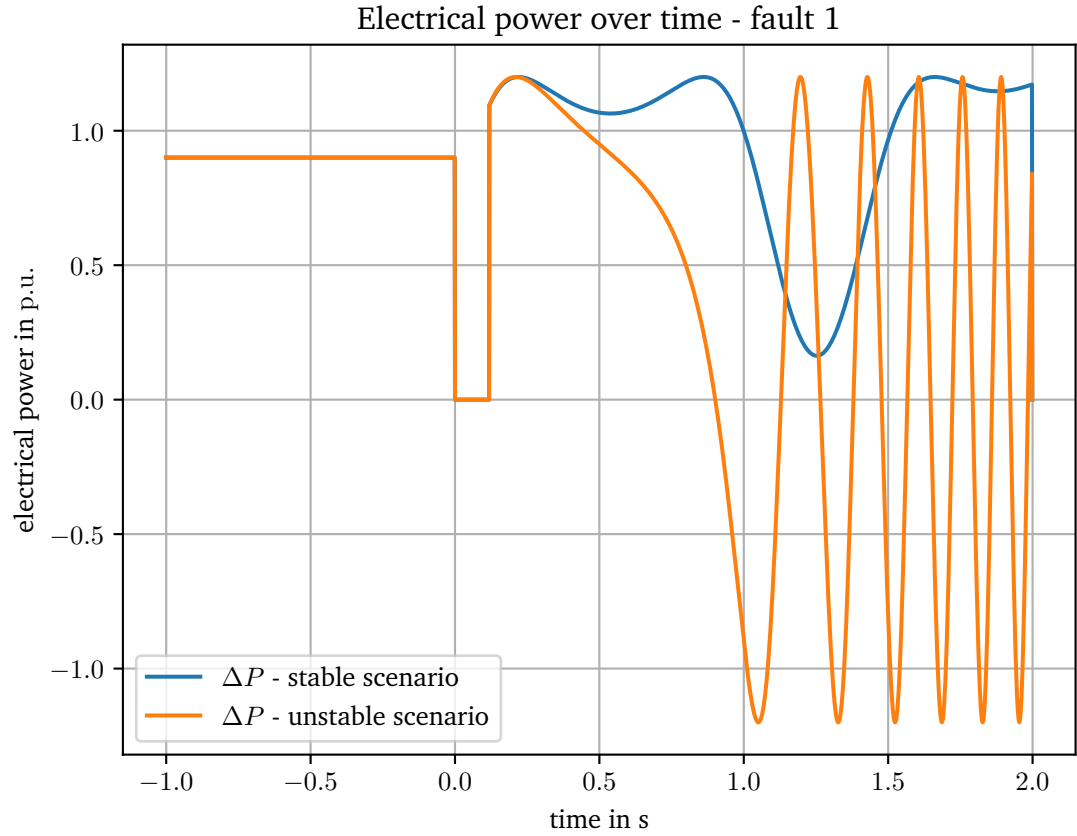
Stable scenario - fault 1





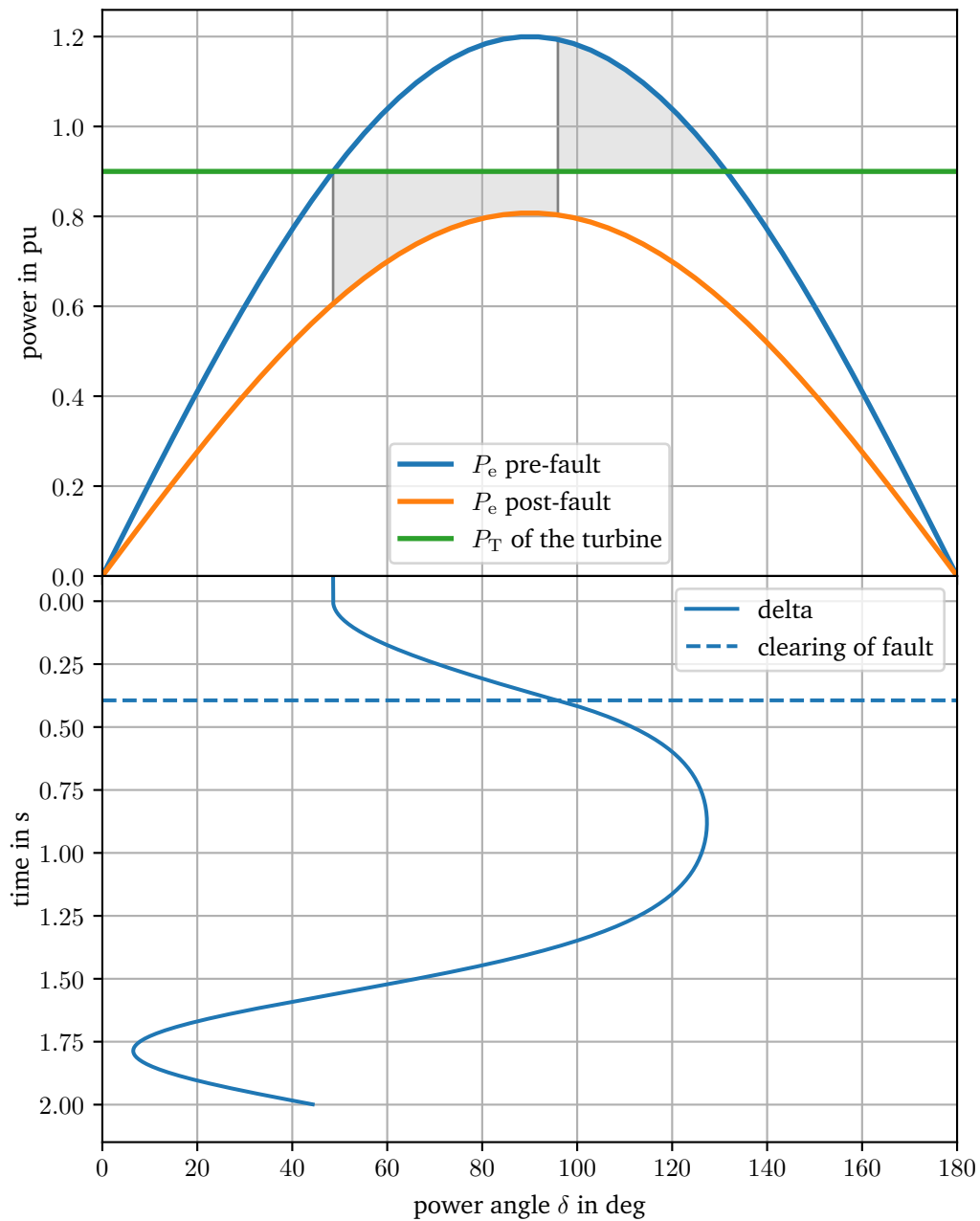
## Unstable scenario - fault 1



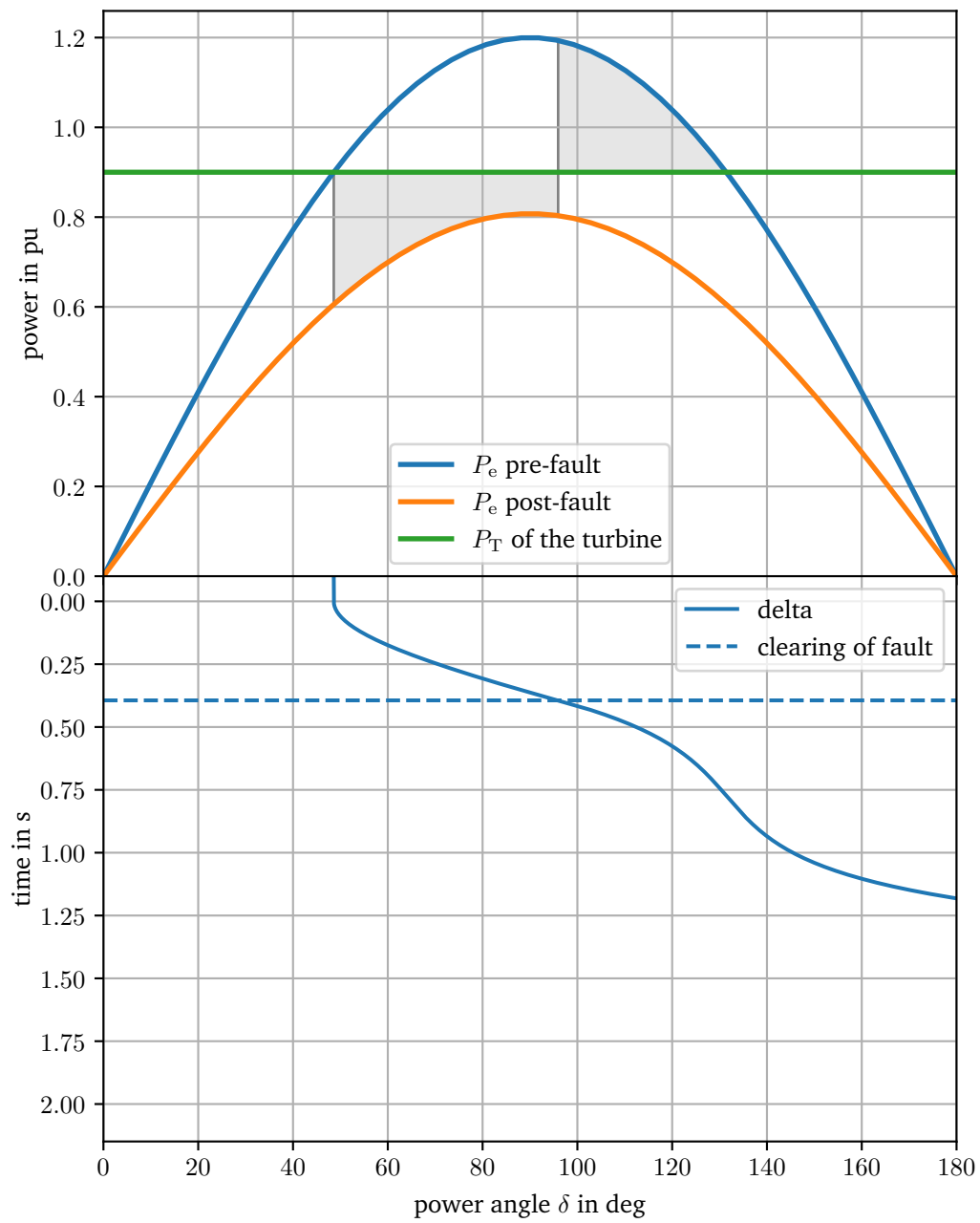


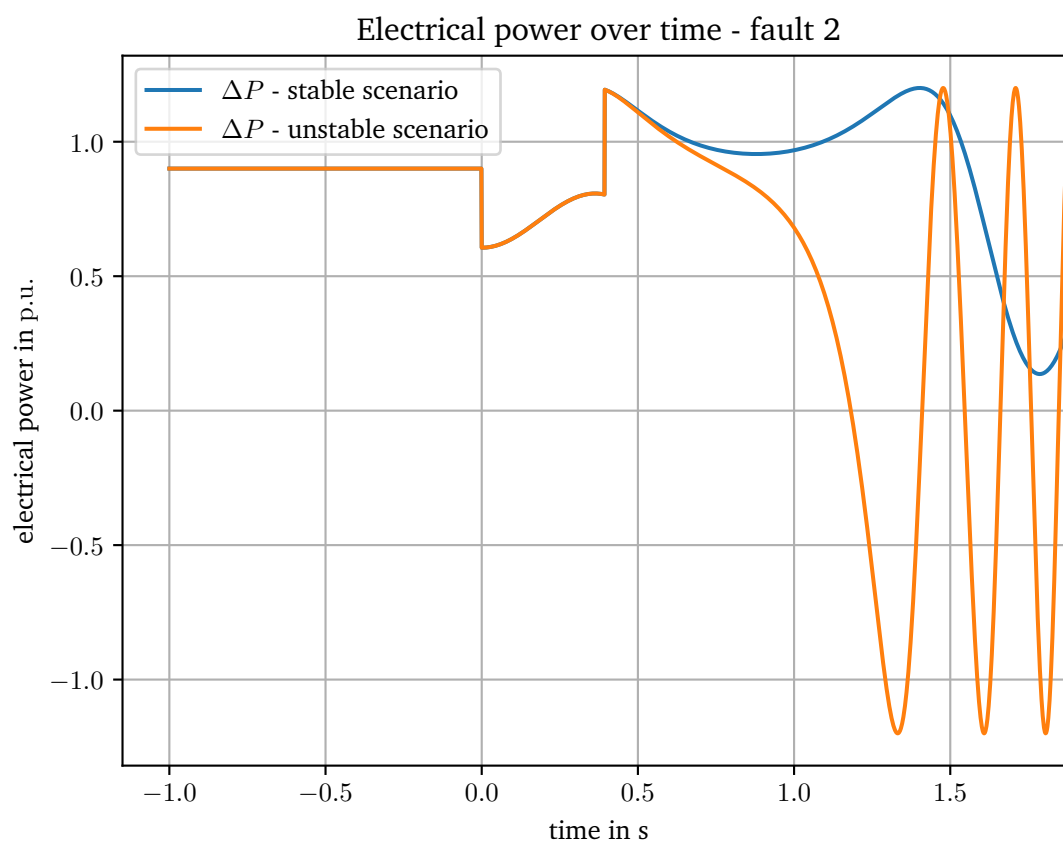
## A.3 Fault 2

Stable scenario - fault 2



## Unstable scenario - fault 2





### A.4 Fault 3

Stable scenario - fault 3

